Construction and Building Materials 49 (2013) 915–925

Contents lists available at SciVerse ScienceDirect

Construction and Building Materials

journal homepage: www.elsevier.com/locate/conbuildmat

Ductility of FRP–concrete systems: Investigations at different length scales

Oguz Gunes [a], Denvid Lau [b], Chakrapan Tuakta [c], Oral Büyüköztürk [d,*]

[a] Department of Civil Engineering, Cankaya University, Ankara, Turkey
[b] Department of Civil and Architectural Engineering, City University of Hong Kong, Hong Kong, China
[c] Department of Civil Engineering, Kasetsart University, Bangkok, Thailand
[d] Department of Civil and Environmental Engineering, Massachusetts Institute of Technology, Cambridge, MA, USA

HIGHLIGHTS

- Ductility plays an important role in earthquake resistant design of structures.
- Environmental factors may adversely affect the ductility due to premature failure.
- Characterization of ductility at different length scales is described.
- Discussion covers from the continuum regime to the atomistic level.

ARTICLE INFO

Article history:
Available online 3 January 2013

Keywords:
Ductility
Concrete
FRP
Debonding
Fracture
Moisture
Temperature
Multi-scale

ABSTRACT

Fiber reinforced polymer (FRP) materials have been increasingly used in the last two decades to improve various structural characteristics of reinforced concrete (RC) bridges, buildings and other structures. Ductility of the resulting FRP–concrete system plays an important role in structural performance, especially in certain applications such as earthquake resistant design of structures, where ductility and energy dissipation play a vital role. Wrapping RC columns with FRP has been shown to generally result in significant increase in ductility due to the confinement of concrete by the FRP. Other applications such as flexural strengthening of beams involve tradeoffs between ductility and the desired load capacity. Furthermore, environmental factors may adversely affect the FRP–concrete bond raising concerns about the ductility of the system due to possible premature failure modes. Characterization of these effects requires the use of more involved mechanics concepts other than the simple elastic or ultimate strength analyses. This paper focuses on characterizing ductility of the FRP–concrete systems at different length scales using a combined experimental/computational mechanics approach. Effects of several parameters on ductility, including constituent material properties and their interfaces, FRP reinforcement geometry at the macro- and meso-level, and atomistic structure at the molecular level are discussed. Integration of this knowledge will provide the basis for improved design strategies considering the ductility of FRP–concrete systems from a global as well as local perspective including interface bond behavior under various mechanical and environmental conditions.

1. Introduction

Fiber reinforced polymer (FRP) composite materials have been increasingly used to improve the load capacity and serviceability of reinforced concrete (RC) members and structures in the last two decades. Despite many favorable properties of FRP composites that encourage their use in conjunction with RC structures, a key concern is their typical brittle failure following a linearly elastic stress–strain behavior [1]. The current transition in design codes towards performance-based design and evaluation procedures places increased emphasis on the deformation and ductility behavior of structures for satisfactory structural performance. Hence, accurate assessment of the ductility characteristics of FRP–concrete systems at different scales as affected by major influential factors is a necessity to ensure their safety throughout the intended service life.

This paper focuses on the ductility of FRP–concrete systems based on investigations ranging from the structural- to nano-scale involving atomic-scale simulations. The paper begins with the definition and significance of ductility in the design and evaluation of new and existing structures followed by a discussion of the ductility characteristics of FRP–concrete systems at different scales as affected by various factors. The scope is limited to use of 'FRP as

* Corresponding author.
E-mail address: obuyuk@mit.edu (O. Büyüköztürk).

0950-0618/$ - see front matter © 2012 Elsevier Ltd. All rights reserved.
http://dx.doi.org/10.1016/j.conbuildmat.2012.10.017

external reinforcement in concrete', which is one of the four major types of FRP–concrete systems defined in the relevant ACI 440 publication [2]. The investigations at the structural scale are presented from a seismic performance perspective due to greater emphasis on ductility as a performance measure in seismic design. Due to the typical sizes of civil infrastructure components such as buildings and bridges, previous research on ductility has usually been conducted at macro-scale and those at meso- and nano-scales are limited. In this paper, quantitative discussions of ductility are presented also in the smaller length scales through both experimental and simulation approaches. It is expected that such fundamental understanding of ductility across different scales in a bonded system will be valuable for development of better design strategies.

2. Significance of ductility in design and evaluation of structures

Ductility of a structural system, its components, and the constituent materials has always had special importance in the design of structures. Defined – at different scales – as the ability to undergo inelastic deformation before failure, ductility not only results in warning before ultimate failure but also it reduces the dynamic load demand through increased energy dissipation and damage. The latter phenomenon has had a profound significance in the design of structures in seismic regions for at least the last half a century. The experience and observations during this time have verifiably demonstrated that structures can be economically designed considering only a fraction of the calculated elastic seismic design loads without violating the safety and performance objectives [3,4]. Allowing ductility-enabled inelastic deformation and damage in the structure, this design philosophy has been widely implemented by the code-use of a Seismic Response Modification Factor, R, to reduce the elastic seismic loads (V_E) to seismic design loads (V_S) as shown in Fig. 1a [5]. This reduction implicitly relies on the ductility (μ) expressed by the ratio of the ultimate drift (Δ_u) and the yield drift (Δ_y) shown on the bilinear approximation to the capacity curve in the figure. For design purposes, the design shear (V_S) is magnified by the overstrength factor, Ω, considering force controlled members, and the drift (Δ_S) is magnified by the deflection amplification factor, C_d, to realistically satisfy the drift limitations for satisfactory seismic performance. Hence, even though the design requirements are stated in terms of forces and the design is based on elastic analysis, the traditional seismic design philosophy is rooted in the expected inelastic deformation and ductility behavior of structures.

An alternative design approach proposed to replace the traditional seismic design methods is the Yield Point Spectra (YPS) representation of the seismic demand which allows convenient graphical superposition of the ductility and drift limits as shown in Fig. 1b [5,6]. Applicable to design and evaluation of new and existing structures, respectively, this design approach calculates the base shear required to limit ductility and drift demands based on an estimate of the yield displacement and uses a plastic mechanism analysis to calculate the required member load capacities. The transition in the code design approaches is in parallel with the developments in the performance-based evaluation and design procedures that put greater emphasis on the inelastic deformation and ductility behavior of structures to characterize seismic demand and performance.

Evaluation of an existing structure for seismic performance assessment and possible retrofitting is relatively less flexible than design of a new building since the structural system is fixed and typically the available information is limited. The evaluation procedure generally involves nonlinear static pushover analysis [7,8] of the structure to obtain the capacity curve and estimation of the corresponding seismic demand to determine the peak displacement response. Ductility of the system and its constituents at various scales play a vital role in the seismic performance level. Fig. 2 shows the ductility characteristics and measures at the scale of structures, members, and constituent materials for an RC structure. At the scale of a structure (typically 10^{1-2} m), the total base shear – roof displacement/drift (V–Δ) relation defines the capacity curve for the structure which leads to its seismic performance. The measure of ductility at the structural scale is the ratio of the ultimate drift (Δ_u) and yield drift (Δ_y) identified on the bilinear approximation to the capacity curve in Fig. 2a. At the scale of members or components (typically 10^{0-1} m) the force–deformation relationship is generally expressed – from a computational perspective – in terms of moment–rotation (M–θ) relation obtained from the moment–curvature (M–φ) relation using the estimated plastic hinge length (L_p). Measures of ductility at the scale of members and components include the ratio of ultimate curvature or rotation (φ_u, θ_u) and yield curvature or rotation (φ_y, θ_y), respectively, as shown in Fig. 2b. The load deformation behavior of members and structures are determined by those of the constitutive materials that make up the member section (typically $10^{(-1)-(0)}$ m) at macro-scale (typically $10^{(-2)-(-1)}$ m). The measure of ductility at the scale of materials is the ratio of the ultimate strain (ε_u) and the yield strain (ε_y) as shown in Fig. 2c for reinforcing steel and concrete. While the ductility ratio (μ) of reinforcing steel typically exceeds 100, that of normal strength concrete (under compression) is only about 2 using a bilinear approximation to the stress–strain curve according to Eurocode 2 [9]. Composite use of these two materials in a complementary fashion and proper design of the members aim at producing a safe and economical structure with

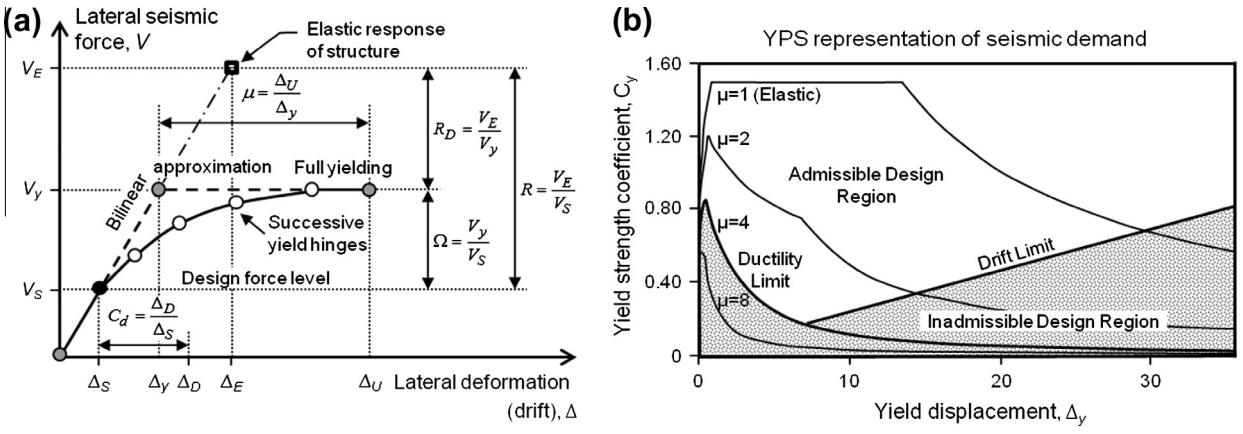

Fig. 1. Significance of inelastic deformation and ductility in structural design (adapted from [5]).

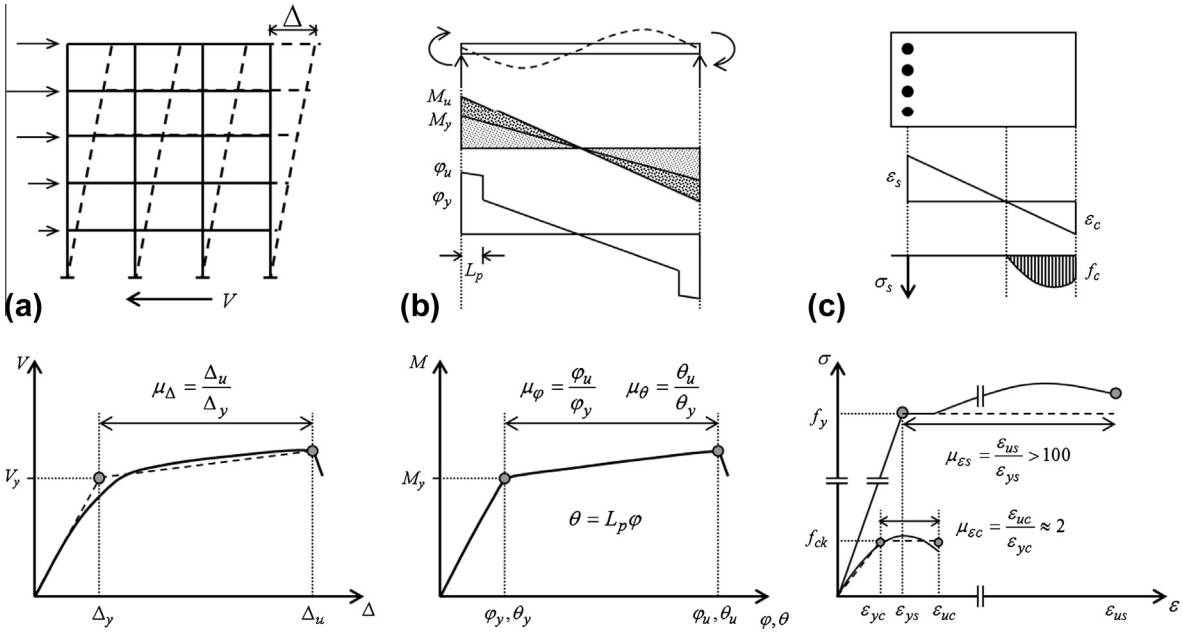

Fig. 2. Ductility measures for (a) structures, (b) members and (c) constituent materials.

satisfactory seismic performance, which rarely requires a system level ductility supply of 4–6 for typical structures [4].

3. Ductility characteristics of FRP–concrete systems at different scales

3.1. Investigations at structural level

FRP composite materials have several favorable properties that justify their use in concrete structures. Among these are the high strength and stiffness to weight ratios, tailorable material properties and geometry, ease of application, and exceptional durability against environmental and mechanical effects. In view of the discussions in the preceding section, however, certain characteristics of FRP materials and FRP–concrete systems cast doubts about their suitability for use in concrete structures. From the ductility perspective, the most significant concern is the linearly elastic tensile stress–strain behavior followed by a brittle failure common to most FRP composites. The fundamental problem in this respect is the use of (mostly uniaxial) FRP with a ductility ratio of $\mu \approx 1$ [1] in addition to steel and concrete shown in Fig. 2c, which at first look does not promise a favorable contribution to the system ductility. A partially compensating property of FRP composites is their typically much higher ultimate strain ($\varepsilon_{uf} \approx 0.012$–$0.023$) compared to that of concrete ($\varepsilon_{uc} \approx 0.003$) and the yield strain of reinforcing steel ($\varepsilon_{ys} \approx 0.002$) [1]. Since the ductility of reinforcing steel in a properly designed RC member is never fully realized due to concrete failure, the additional FRP reinforcement – if properly designed and installed – does not alter the failure mode and acts as additional reinforcement to increase the load capacity and/or ductility depending on the application [10].

Fig. 3 shows the influence of FRP strengthening on the load–deformation behavior of beam and column elements. In the figure, the shaded areas above the load–deformation curves before strengthening show the conceptual domain of typical responses after strengthening. When presenting experimental results, load–deformation curves are often preferred as shown in the figure, but these generally need to be converted to moment–curvature/rotation relations shown in Fig. 2b for pushover analysis. For under-reinforced beam elements, bonding FRP reinforcement to the soffits and/or top surface along the positive and negative moment regions, respectively, can improve the beam's flexural capacity. This capacity increase, however, is generally accompanied by a reduction in the beam's ductility as conceptually illustrated in Fig. 3 (left) [10,11]. FRP acting as additional flexural reinforcement results in earlier crushing of concrete in compression, reducing

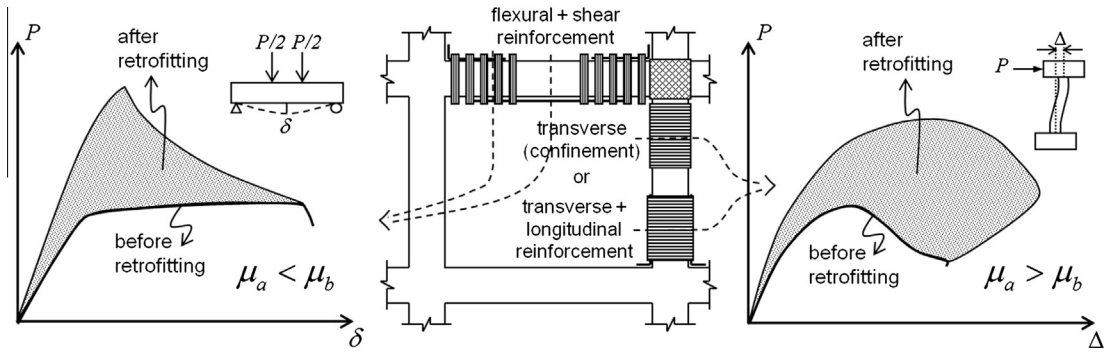

Fig. 3. Typical influence of FRP retrofitting on the load capacity and ductility behavior of beam and column elements. In the figure, μ_a refers to "after strengthening" and μ_b to "before strengthening".

the deformation capacity. The trade-off between flexural capacity and ductility in FRP strengthened beam elements is an important design consideration that may influence structural performance.

FRP strengthening of columns has been the most successful application of FRPs to RC structures. Unlike the beams, FRP strengthening of columns generally result in an increase in the column ductility as illustrated in Fig. 3 (right). This is due to the additional confinement of concrete by the transverse FRP reinforcement which increases both the compressive strength and ultimate strain of concrete [12,13]. When column retrofitting is limited to FRP wrapping of column ends to act as transverse reinforcement for additional confinement, the typical response under lateral loading is a significant increase in the member ductility with a modest increase in the lateral load capacity [14]. This type of retrofitting is performed for ductility enhancement and the increase in load capacity is sometimes ignored in design for simplicity [15–17]. When the objective is to increase the lateral load capacity of columns, both transverse and longitudinal FRP reinforcement is used for strengthening and the typical response is an increase in both the lateral load capacity and ductility, although the ductility increase is typically less than that achieved by transverse reinforcement only.

Different orientations of the FRP reinforcement and their stacking sequence were found to have a significant influence on the lateral confining pressure and the corresponding FRP failure stress. Fig. 4 shows the stress–strain behavior and failure of six axially loaded concrete cylinders wrapped with one or two layers of GFRP sheets with three different fiber orientations [18,19]. All FRP wrapped cylinders displayed an improvement in both axial load capacity and ductility compared to the plain concrete cylinder. The degree of improvement and the failure mode were affected by the number of layers, fiber orientation, and the stacking sequence. Fiber orientation may improve in load capacity and ductility due to the participation of the fibers in load carrying capacity in addition to that due to the confinement effect of the FRP. Similar improvements were obtained in lateral load and deformation capacity of FRP wrapped columns [20].

Accumulated knowledge and experience in behavioral modeling of FRP strengthened RC members have led to several recent experimental and analytical studies investigating the performance of FRP strengthened RC frames and subassemblies [16,17,21–25]. FRP strengthened member models combined with the recently developed performance based analysis and design tools allow for analytical investigation of the method's potential for RC frames. Fig. 5a shows an RC frame model assumed to be retrofitted through FRP strengthening of beams for improved flexural capacity and/or wrapping of columns as shown in Fig. 5b for additional confinement and resulting ductility [26]. Fig. 5c shows the idealized moment–rotation relations normalized with the yield moment (M_y) obtained from moment–curvature analyses using confined concrete models by [27] and by [13] for steel and FRP confined concrete sections, respectively. Fig. 5d shows the capacity curves for the frame before and after retrofitting the beam and/or column elements. As can be seen from the figure, FRP wrapping of columns only increases the deformation capacity and ductility of the frame without significant increase in its lateral load carrying capacity. FRP strengthening the beams in addition to columns results in an increase in the frame's lateral load capacity, but this happens at the expense of partial deformation capacity, resulting in relative loss of ductility compared to retrofitting columns only. Significance of the FRP retrofit scheme and the resulting ductility behavior in terms of seismic performance is shown in Fig. 5e using the Capacity Spectrum Method [28] in the acceleration–displacement response spectrum (ADSR) format as initially described in the ATC-40 report [7] and later improved in ATC-55 [8,29]. As shown in the figure, the bare frame before retrofitting does not have an intersection with the corresponding seismic demand curve, which means that the bare frame is likely to collapse under seismic design loads. Retrofitting the columns significantly improves the ductility of the structure and a performance point is obtained. If the corresponding ductility and drift demand exceed the code specified limits, as conceptually illustrated in Fig. 1b, then one needs to strengthen the beams in addition to columns to obtain the performance point at a lower drift value. As shown in Fig. 5e, strengthening both columns and beams shifts the performance point to the left, but reduces the ductility of the retrofitted frame. With the described tools at hand, it is the responsibility of the designer to optimize the retrofit scheme to obtain satisfactory structural performance at a reasonable retrofit cost.

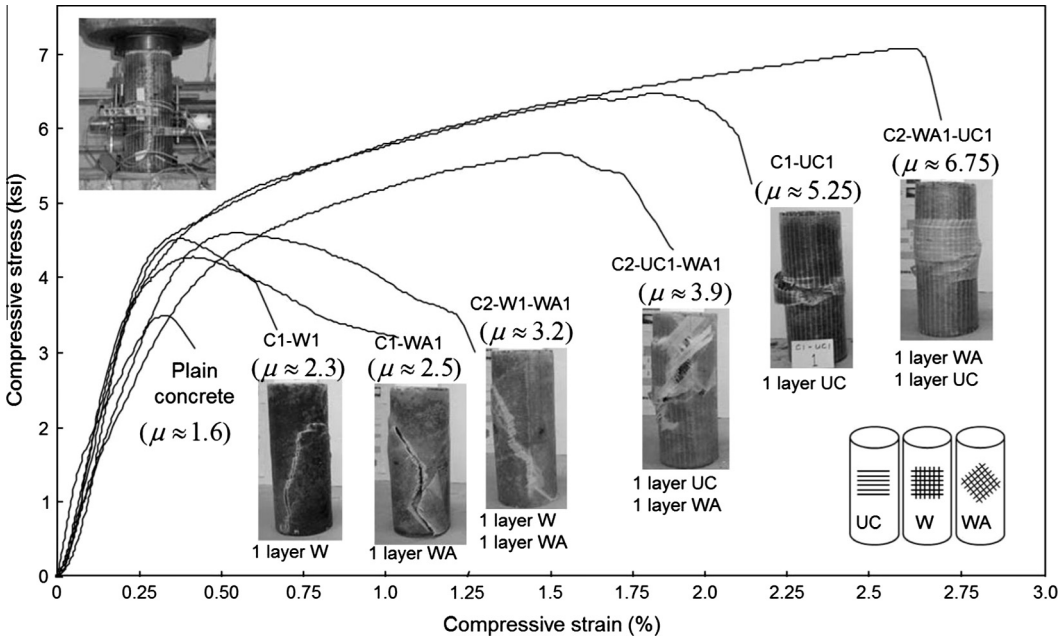

Fig. 4. Failure behavior of GFRP wrapped concrete cylinders under axial compression.

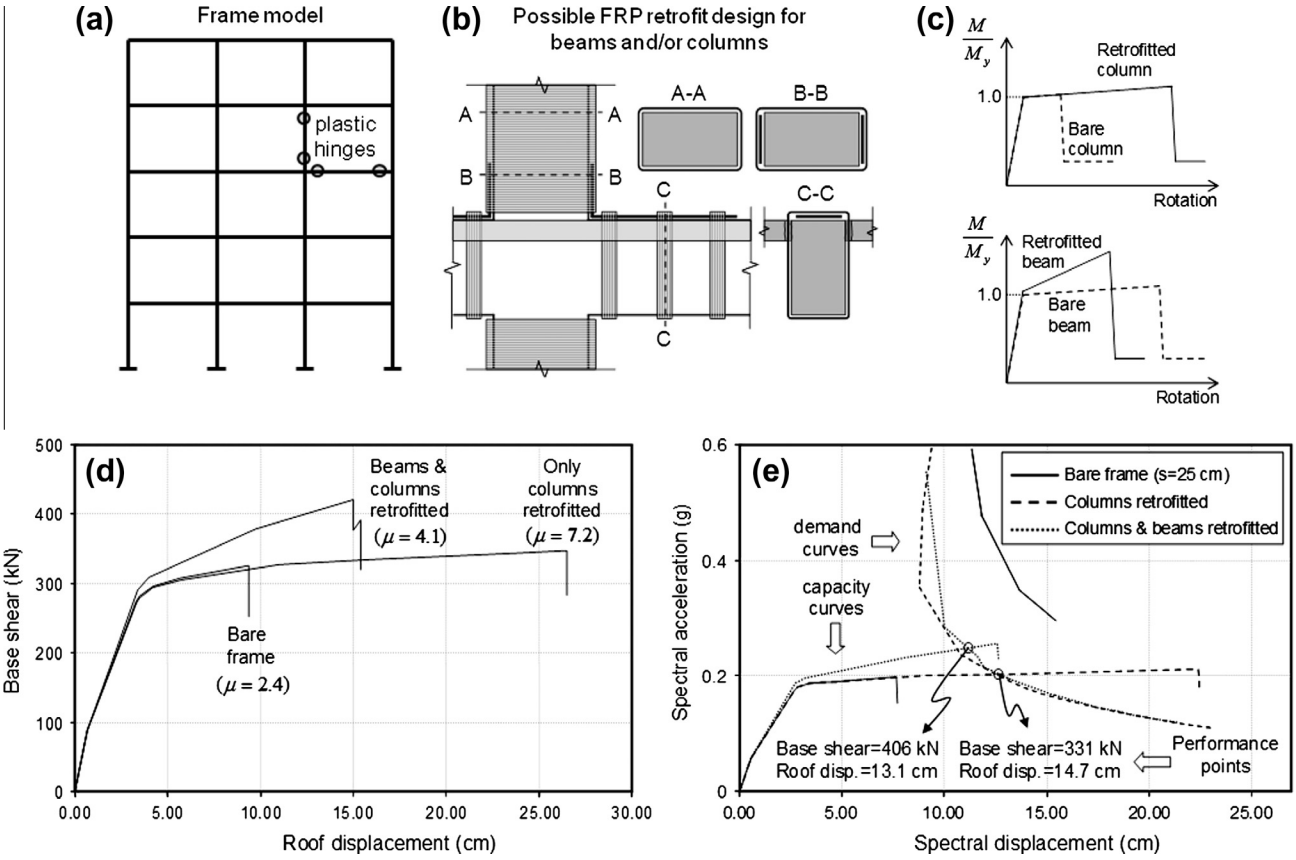

Fig. 5. Lateral load capacity and ductility behavior of an RC frame upon FRP retrofitting.

3.2. Investigations at meso-scale level

The above FRP related ductility improvements are based on the assumption that the FRP–concrete interfaces are always intact. In case of FRP confinement, ductility improvement can be achieved as long as there is contact between concrete and FRP to provide a required level of lateral pressure [30]. On the other hand, studies have shown that ductility, durability, and debonding of interfaces significantly affect the strength and deformation behavior of flexural strengthening system and may result in new and undesirably less ductile failure modes. In this section, strength and ductility of the FRP–concrete interface is discussed. In addition to material properties, failure behavior of FRP-retrofitted RC flexural elements significantly depends on the properties of the interface between concrete and FRP, in which interface comes into play as an additional structural component influencing ductility and failure. Note that the following discussion pertains to FRP retrofit of flexural RC elements, where bond performance is critical.

Integrity of FRP–concrete systems and the influence of interface properties on system ductility and failure behavior can effectively be characterized using fracture mechanics concepts. In this approach the major quantification parameter is the critical fracture toughness of the interface. FRP–concrete bond joints, such as those in FRP-strengthened RC beams, can be idealized as a three-layered material system consisting of concrete, epoxy and FRP. In such a system, crack can propagate in five regions—bulk concrete, FRP sheet, bulk epoxy, the interface between concrete and epoxy, and the interface between epoxy and FRP (Fig. 6). Using energy considerations, the energy release rate can be computed from the difference in the strain energy of the cracked body (far behind the crack tip) and that of the intact body (far ahead of the crack tip). The detailed derivation of the tri-layer fracture toughness is given in [31]. The expression of the energy release rate contains geometric and material information of all the three material layers. To obtain the fracture toughness of the system from the experiment, configurations of meso-scale peel and shear fracture specimens were chosen to represent possible loading cases found in a full-sized FRP-strengthened concrete beam as shown in Fig. 7a. The opening (mode I fracture) and shearing (mode II fracture) loading cases are represented by the peel and shear specimens as shown in Fig. 7b. To compute the interface fracture toughness of the FRP/concrete bond system, critical loads obtained from the debonding tests and the material properties obtained from the material characterization were used.

Fig. 8a and b shows typical load–displacement curves of the meso-scale peel and shear fracture tests, respectively. For both types of tests, load increases almost linearly as the displacement at the end of FRP cantilever arm increases until crack propagation initiates. After that point, load–displacement curves of peel fracture test show stepwise decrease until complete failure. This corresponds to stepwise propagation of the crack front. The load at crack initiation of each consecutive step is, in general, less than that of the previous step. This is because the length of FRP cantilever arm increases at every step. Hence, smaller force is required to generate moment sufficient for crack propagation. On the other hand, shear fracture test shows almost a linear drop in load after crack initiation and a sudden cut-off, which corresponds to FRP plate being completely removed from the specimens. The non-linearity near the peak load in the load–displacement curve of the shear fracture test implies that material in the vicinity of the crack has already reached its elastic limit, and strain energy has partially been converted into plastic strain energy. As a result, fracture behavior of FRP–concrete interface in mode II displays higher ductility than that in mode I due to plasticity. Nonetheless, if the relative displacement at ultimate failure and crack initiation are considered instead, fracture behavior

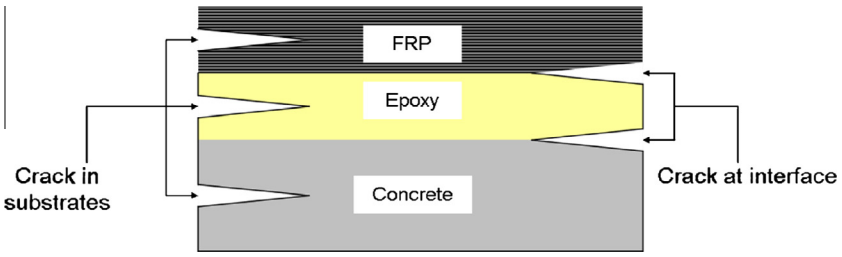

Fig. 6. A tri-layer system consisting of concrete, epoxy, and FRP.

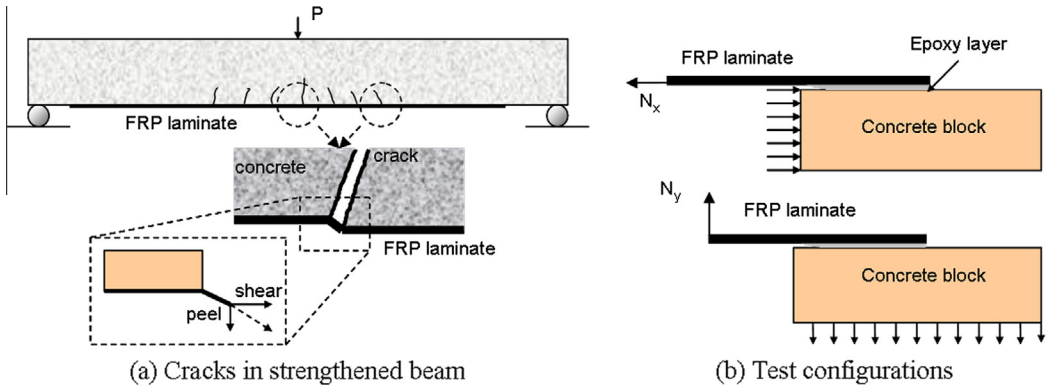

Fig. 7. (a) Idealization of loading state in FRP in the vicinity of a crack; (b) peel and shear fracture specimens for opening and shearing modes of loading.

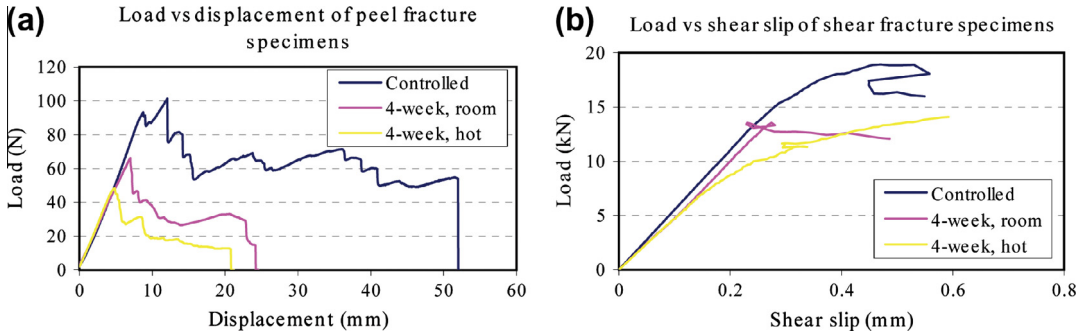

Fig. 8. Typical load–displacement relationship of meso-scale peel and shear fracture specimens.

of FRP–concrete interface in mode I is more ductile in this regard. If debonding failure was to occur in FRP-strengthened RC beam due to environmental degradation, for example, it was more likely that failure would be more gradual when mode I fracture dominated. Mode I fracture generally exist in combination with mode II within the shear span due to relative crack mouth opening, while mode II fracture dominates at the plate-end. Therefore, provision of anchorage at the plate-end is very important when FRP strengthening system is to be used in a severe environment in order to avoid brittle failure due to mode II debonding. It is worth noting that the ductility ratio of the FRP–concrete interface under shear maybe estimated as the ratio between the shear slip at ultimate failure of the interface to the shear slip at first yield of the epoxy. This gives ductility values in the range of 2–3 from the test, which is higher than that of concrete. It is interesting to observe from Fig. 8 that the peak loads of peel and shear fracture specimens exposed to 4 weeks of moisture conditioning are lower than those of the dry specimens. Moisture effects will be further discussed in Section 4.1.

3.3. Investigations at nano-scale level

Although classical fracture mechanics enables one to quantify the interfacial deterioration through the critical fracture toughness, it does not provide any insight into what is actually happening at the vicinity of the interfacial crack. As a more fundamental approach at the molecular level, molecular dynamics simulation has been adopted for studying the interaction of materials at the interface. In this section, we describe a new approach using the concept of free energy for measuring the load–displacement response of the bonded system at the nano-scale level, at which the fluctuation of the response can be reduced. This approach is demonstrated using epoxy–silica bonded system as an example, in which the interface is dominated by relatively weak van der Waals forces and Coulombic interactions. Here, silica is chosen as a representative material for concrete because it is a commonly found material in nature in the form of sand or quartz and is the major constituent material in concrete (about 40% by mass). It is believed that the epoxy–silica interface is representative of the FRP–concrete bonded system and the investigation on the ductility of epoxy–silica system can form the basis for future studies on ductility of FRP–concrete systems with the consideration of the heterogeneous nature of concrete at nano-scale.

The first step of this new approach is the reconstruction of the free energy surface (FES) which describes the energy change in the epoxy–silica system from an attached stage to a detached stage. Such reconstruction becomes feasible by using the metadynamics approach [32,33] which is a powerful algorithm that can be used

for both reconstructing the free energy and for accelerating rare events in the system. The principle of this algorithm can be qualitatively understood by filling the actual FES by a series of external energy with a Gaussian distribution. By keeping track of the filled Gaussians, the FES can be calculated. In other words, the debonding process is initiated by an external energy source with a Gaussian distribution of energy which is continuously added to the bonded system and hence the entire process does not involve any direct application of an external load to the system. It should be mentioned that the debonding mechanism of the bonded system captured from the FES is homogenous as shown in Fig. 9a and is not likely to represent the detachment mechanism when a single epoxy chain is separated from the silica surface by a mechanical load acting at the far end of the epoxy chain. It is believed that the nano-scale debonding mechanism can be regarded as homogeneous when such debonding is initiated at macro-scale structural level.

After obtaining the FES between epoxy and silica from molecular dynamics simulation as shown in Fig. 9b, the load–displacement response as shown in Fig. 9c can be predicted by considering the first derivative of the FES. Fig. 8 summarizes the approach qualitatively. The reader is referred to [34,35] for more detailed information on his approach.

The molecular dynamics simulation results show a softening behavior in the load–displacement response once the peak stress is reached (Fig. 9c). It is mainly because the interactions between epoxy and silica at nano-scale are governed by the weak van der Waals and Coulombic forces which do not allow any plastic shear deformation to occur in the post-peak regime of the load–displacement curve. The ductility ratio (μ) in the nano-scale epoxy–silica bonded system can be defined as the ratio between the total area under the load–displacement curve (energy per unit area = 569 nJ/mm^2) and the elastic energy per unit area (60.5 nJ/mm^2) which is calculated as $\mu = 9.4$. Such a high ductility ratio cannot be observed at macro-scale structural level in general since the weak van der Waals and Coulombic forces become extremely insignificant when the separation is more than few nanometers. Hence, the ductility will generally decrease from nano-scale to macro-scale if the bonded systems lack meso-scale material features (e.g. surface roughness leading to mechanical interlock, confinement effect) which can lead to significant energy dissipation to occur at the interface.

3.4. Ductility insights from various length scale viewpoint

For an FRP-bonded concrete system, multi-scale investigations indicate that the ductility generally displays a decreasing trend from nano-scale to macro-scale level. At nano-scale, the van der Waals forces and Coulombic interactions are still significant in which certain portion of energy can be dissipated during the debonding process (e.g. sliding of epoxy chain on the concrete substrate). However, at the sub-micro-scale level, such interaction becomes insignificant and the bonded system can be very brittle if there is no other means to dissipate energy during debonding. It is the reason why little ductility can be observed at the meso-scale with ductility values calculated in the range of 2–3 from the tests. At the structural scale, the failure is not solely governed by the interfaces of the FRP-bonded system. Various deformation mechanisms can be involved at this scale, which lead to significant energy dissipation during the deformation process, such as the confinement effect in the column and the mechanical interlock between concrete and epoxy in the FRP retrofitted RC beam. Therefore, even though FRP itself does not possess any ductility, the ductility of the entire bonded system can still be within an acceptable level by introducing appropriate energy dissipation mechanisms when the system is beyond its elastic limit. This requires implication of efficient design strategies at the structural level.

It should be mentioned that the above discussion is founded on the basis that the system failure is initiated by the local debonding at the interface between the adhesive and the concrete substrate. Such an interface becomes the most critical region when the FRP-bonded concrete system is subjected to prolonged moisture and elevated temperature as reported in various research studies [31,36,37]. Recently, the use of a higher elongation ductile resin system as adhesive has been proposed for the ductility improvement of the FRP-bonded concrete systems [38,39]. However, the long term performance of a ductile adhesive material in FRP-bonded concrete systems still remains unanswered. Further investigation is required to understand how the ductility changes across different length scales using ductile adhesive materials.

4. Factors affecting ductility of FRP–concrete systems

The discussions in the preceding sections illustrate the ever increasing importance of ductility in structural evaluation and design of FRP–concrete systems through investigations at different length scales. Implicit in these discussions, however, are a number of assumptions that idealize or disregard the potential influence of various factors that may affect the ductility behavior of FRP–concrete systems at all length scales. Some of these factors are related to the design issues. For instance, the FRP strengthened member behaviors conceptually illustrated in Fig. 3 cannot be migrated to the structural scale evaluations shown in Fig. 5 without considering and ensuring satisfactory performance of beam-column joints [40–42]. Other factors are related to the performance of materials and their interfaces under mechanical effects, such as premature debonding failures that may significantly reduce structural ductility and performance unless adequate bond or mechanical

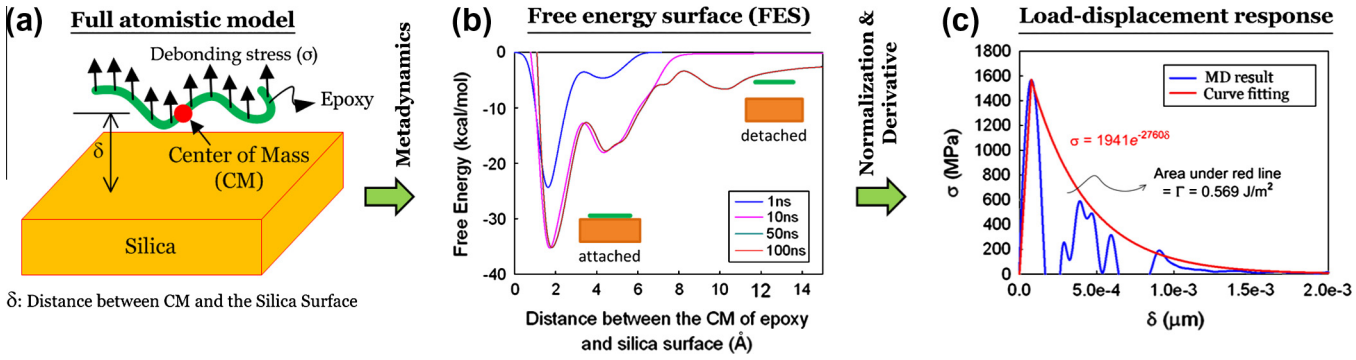

Fig. 9. Illustration of the process of using molecular dynamics simulation (a) to determine the free energy surface (b) using advanced molecular dynamics methods such as Parrinello's metadynamics (to sample for rare events while reconstructing the FES), to identify (c) the load–displacement response of the bonded system.

anchorage of the FRP reinforcement is ensured. Materials and interfaces are also susceptible to the moisture and chemical effects of environmental exposure that may alter the chemistry and mechanical behavior of constituent materials and interfaces. Additional factors may include electrochemical effects such as the corrosion of internal steel reinforcement which may reduce the effectiveness of external FRP reinforcement and hence the ductility of the system.

4.1. Effects of moisture on FRP/concrete interface

Using fracture test configuration discussed in Section 3.2, it was found that prolonged exposure to moisture condition may result in significant degradation of the FRP–concrete bond strength as shown in Fig. 10 [36]. More than 50% of the initial bond strength can be lost by exposure to moisture, even after a duration of only two weeks. Degradation can be as much as 70% for specimens conditioned for 8 weeks. After a certain period of time, the bond strength approaches a certain value, with no further significant degradation thereafter. This asymptotic fracture toughness is the minimum bond strength an FRP–concrete bonded system can retain after a very long moisture exposure. Exposure to moisture combined with higher temperature results in slightly lower bond strength after the same period of moisture conditioning. For both peel and shear fracture specimens, a shift is observed in the failure mode from concrete delamination in dry specimens, to epoxy–concrete interface separation in wet specimens, at both room temperature and 50 °C indicating a significant weakening of the interface due to the presence of moisture. Similar weakening effect on the FRP–concrete bond system has also been observed for the case of cyclic moisture condition [36].

4.2. Effect of interface degradation on ductility of FRP-plated RC beams – a finite element simulation study

The effectiveness of FRP-strengthening system for flexure depends on the ability of adhesive to transfer load from concrete beam to FRP. If the FRP–concrete interface is weakened due to environmental effects, unexpected premature failures may occur. For example, debonding may take place before yielding of steel reinforcement, causing FRP-plated RC beam to abruptly lose its load capacity. To further study the influence of interface degradation on the behavior of FRP-strengthened flexural members, a finite element (FE) model was created for a laboratory-size FRP-plated beam specimen. Damage plasticity model with tension-stiffening was used for concrete to capture nonlinear behavior in both tension and compression regimes, while bi-linear elastic–plastic models were used to simulate yielding behavior of epoxy and steel reinforcement. Concrete, epoxy, and CFRP were modeled using 4-node quadrilateral plane-strain elements with plane-strain thicknesses of 150 mm for concrete, and 52 mm for the epoxy layer and the CFRP plate. The interface between the concrete and the epoxy layer was modeled by a single layer of 4-node cohesive elements with a uniform meshing throughout the entire length of the bond line. The total length of the interface layer was 625 mm for the half-beam FE model.

The linear traction–separation law for the cohesive elements representing the epoxy–concrete interface in this study requires two types of parameters, namely the cohesive normal and shear strength (t_n^0 and t_s^0) and the mode I and mode II fracture energy (G_{Ic} and G_{IIc}) of the interface. These parameters were obtained from the meso-scale peel and shear fracture tests discussed previously by performing a parametric study with t_n^0 and t_s^0 as the unknown

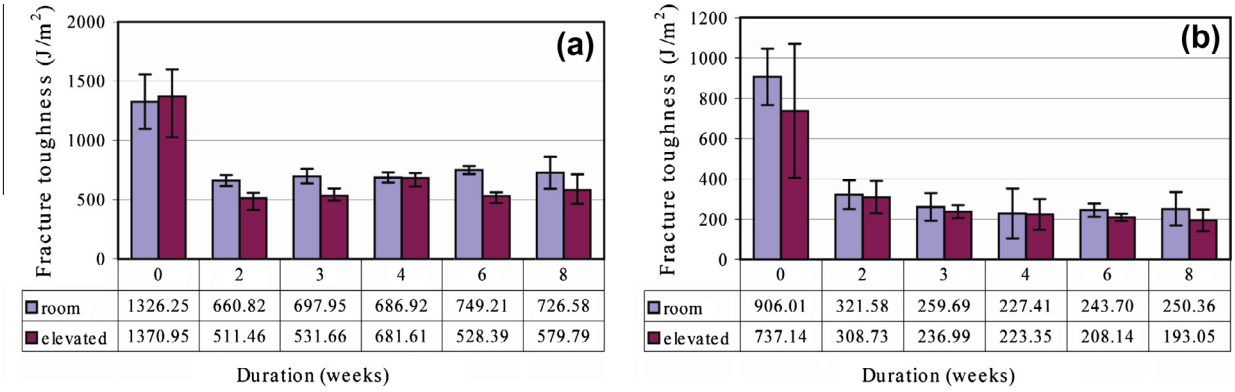

Fig. 10. Effect of moisture on bond strength of shear (a) and peel (b) specimens.

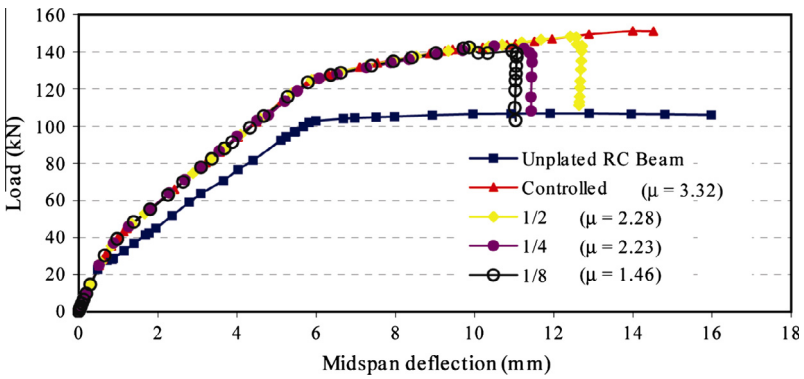

Fig. 11. Effect of Mode I interface properties on debonding behavior of FRP-plated RC beam.

variables. For each moisture conditioning period, the values of cohesive strength were varied until the maximum debonding load was obtained, while the corresponding values of G_{Ic} and G_{IIc} were obtained from the experiments. The values corresponding to dry case were $t_n^0 = 6.1$ MPa, $t_s^0 = 13.92$ MPa, $G_{Ic} = 900$ N/m, and $G_{IIc} = 1300$ N/m. A series of parametric studies were then performed for the beam model by varying the values of t_n^0, t_s^0, G_{Ic} and G_{IIc}. Reduction in the values of these parameters is equivalent to degradation of the concrete–epoxy interface due to environmental exposure. Figs. 11 and 12 show load vs midspan deflection relationships and corresponding ductility ratios when the properties of the interface in mode I or mode II were reduced to 1/2, 1/4, and 1/8 of those for controlled dry case.

In dry condition, the FRP-plated RC beam has higher stiffness than its unplated counterpart, and ultimately fails by concrete cover delamination. However, when the interface is weakened, Figs. 11 and 12 indicate that ductility of FRP-plated RC beams, as measured by the ratio φ_u/φ_y, decreases as mode I or mode II interface properties (i.e. cohesive strength and fracture energy) are reduced. In most cases, this reduction in ductility corresponds to interface separation after yielding of the steel reinforcement. Once separation starts, the beam significantly loses its capacity. In the case of extensive degradation of the concrete/epoxy interface in mode II (i.e. when interface properties were reduced to 1/8), debonding of the FRP plate is predicted to take place even before yielding of steel reinforcement, rendering FRP-strengthening ineffective (Fig. 12).

5. Debonding failures under mechanical effects

Analysis and design of FRP–concrete systems are generally performed using the conventional approaches that assume perfect bonding between the FRP reinforcement and the concrete substrate. Violation of this assumption would mean loss of reinforcement for flexural members and ineffective confinement for column elements, both of which would have negative impact on the member ductility. Countless studies to date have encountered premature debonding failures especially in flexural members that may not only render the FRP strengthening ineffective, but also may harm the structure by reducing element ductility. Reviews of experimental and modeling studies regarding debonding failures can be found in [1] and [43]. Fig. 13 illustrates the significance of debonding failures in terms of the ductility of beam elements through experimental results obtained from ten beam tests [44]. Each beam was strengthened using the same FRP flexural reinforcement but varied in their shear capacity and anchorage conditions. The transverse load versus the FRP flexural reinforcement strain at mid-span $(P - \varepsilon_f)$ was plotted for illustration. As can be seen from the figure, for the same steel and FRP flexural reinforce-

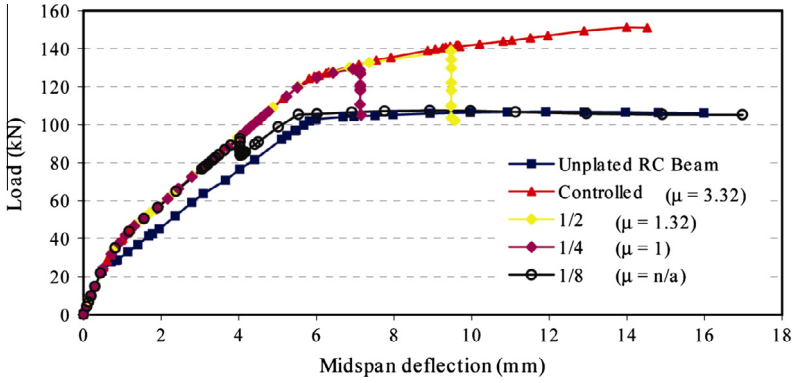

Fig. 12. Effect of mode II interface properties on debonding behavior of FRP-plated RC beam.

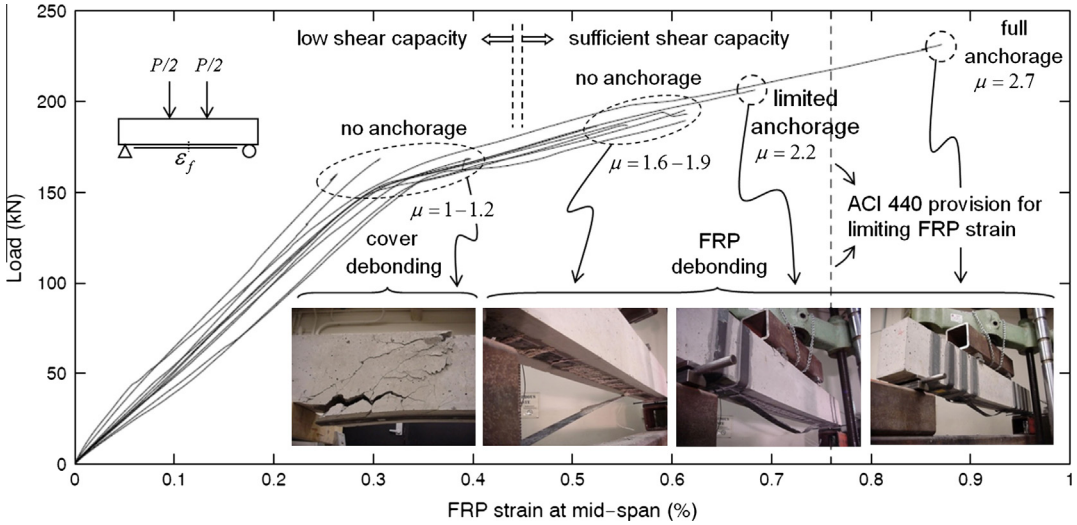

Fig. 13. Influence of debonding failures on the ductility of FRP strengthened beams.

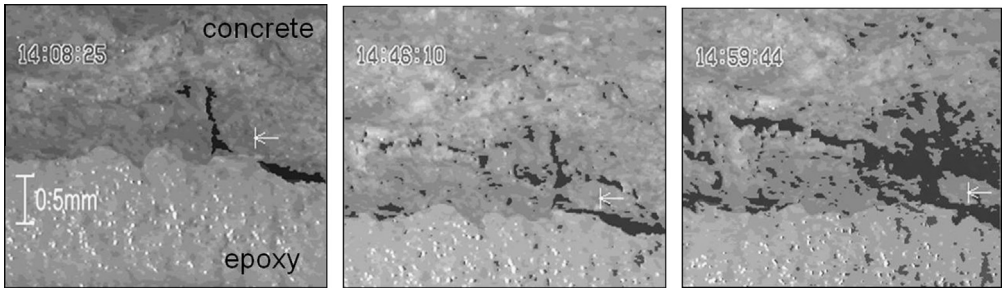

Fig. 14. Damage evolution and debonding propagation at the epoxy–concrete interface.

ment ratio, the ductility ratios of the beams vary between 1 and 2.7 depending on the beam shear capacity and the anchorage conditions, the latter of which cannot be designed using the conventional ultimate strength design approaches.

Different debonding failure modes and associated ductility levels are also shown in Fig. 13 which illustrates the essential design issues in FRP strengthening of flexural members. Cover debonding was the most brittle failure mode which took place at the steel reinforcement level and resulted in a ductility ratio of $\mu = 1–1.2$. Absence of anchorage and insufficient shear capacity were responsible for this brittle failure mode. When adequate shear capacity was provided through additional internal transverse steel reinforcement, the ductility ratio rose to $\mu = 1.6–1.9$ without any bond anchorage. In this case, the failure was at the epoxy–concrete interface, within the concrete substrate. Fig. 14 shows the evolution of debonding damage and propagation at the epoxy–concrete interface [45,46]. Addition of transverse FRP reinforcement for bond anchorage along half and full length of the shear span resulted in ductility ratios of $\mu = 2.2$ and $\mu = 2.7$, respectively. This wide range of ductility behavior may have significant impact on the behavior at the structural scale and requires advanced mechanics tools for modeling and design. A fracture energy based design approach was proposed for bond anchorage design for flexural FRP reinforcement to ensure ductile failure behavior of FRP-strengthened flexural members [43].

6. Knowledge gaps and further research needs

Throughout the paper, discussions on ductility of FRP–concrete systems at different scales were performed with the help of ductility ratios as a quantitative measure of the system's ability to undergo inelastic deformation before failure. Some important observations can be distilled from these discussions that provide guidance for identification of knowledge gaps and further research needs:

- FRP composite materials, due to their favorable mechanical and durability characteristics have secured a permanent and growing share in the construction market with current emphasis on strengthening of RC members. Diverse applications of FRP composites on RC structures enjoy various degrees of success influenced by various material and strengthening parameters.
- From ductility perspective, FRP and concrete materials with ductility ratios approximately $\mu \approx 1$ and $\mu \approx 2$, respectively, do not form an ideal couple considering that higher ductility ratios are required at the structural level for satisfactory structural performance. However, in reinforced concrete applications, existence of reinforcing steel with superior ductility characteristics may result in high system ductility ratio of the FRP–concrete structures. In that respect, more research is needed for better understanding of the interactive system behavior under various mechanical and environmental effects.
- Multi-scale investigations on the ductility of FRP–concrete systems indicate a reduction in ductility at larger scales. This important observation emphasizes the need for more fundamental research at smaller scales to better understand the ductility characteristics of FRP–concrete systems and to optimize material parameters at smaller scales to minimize the reduction in ductility at larger scales.
- Understanding and modeling the influence of moisture, temperature and other environmental exposure conditions on the integrity and ductility of FRP–concrete systems is a priority research area that also concerns the performance and safety of existing FRP–concrete systems. More fundamental research at smaller scales is necessary to properly characterize the coupled chemo-thermo-mechanical processes associated with environmental exposure conditions that adversely affect the integrity, load and failure behavior as well as ductility of FRP–concrete systems in an effort to improve their overall performance.

7. Conclusions

Multi-scale investigations on ductility characteristics of FRP–concrete systems are presented and discussed in this paper sharing the insights gained into mechanics and durability of FRP concrete systems with emphasis on failure behavior and ductility. Knowledge gaps and further research needs are highlighted with emphasis on the need for more fundamental research at smaller scales for better understanding and modeling of coupled mechanisms and processes as a basis for improved design strategies for better performance and ductility.

Acknowledgement

This research was supported by the National Science Foundation (NSF) through the grants CMS Grant Nos. 0010126, 0510797 and 0856325 to Massachusetts Institute of Technology.

References

[1] Büyüköztürk O, Gunes O, Karaca E. Progress review on understanding debonding problems in reinforced concrete and steel members strengthened using FRP composites. Constr Build Mater 2004;18:9–19.
[2] ACI-440. Guide for the design and construction of externally bonded FRP systems for strengthening concrete structures, ACI 440.2R-02. Farmington Hills (MI): American Concrete Institute; 2002.
[3] SEAOC. A brief guide to seismic design factors. Structure Magazine; 2009. p. 30–2.
[4] FEMA. NEHRP recommended seismic provisions for new buildings and other structures: training and instructional materials. Washington (DC): Federal Emergency Management Administration; 2007.
[5] FEMA. NEHRP recommended seismic provisions for new buildings and other structures (FEMA P-750). Washington (DC): Federal Emergency Management Administration; 2009.
[6] Aschheim M, Black EF. Yield point spectra for seismic design and rehabilitation. Earthquake Spectra 2000;16(2):317–35.

[7] ATC. Seismic evaluation and retrofit of concrete buildings (ATC-40). California: Applied Technology Council; 1996.
[8] FEMA. Improvements of nonlinear static seismic analysis procedures (FEMA-440). Washington (DC): Federal Emergency Management Administration; 2005.
[9] CEN. Eurocode 2: design of concrete structures – Part 1-1: General rules and rules for buildings, Ref. No. EN 1992-1-1:2004. E. Brussels: European Committee for Standardization; 2004.
[10] Büyüköztürk O, Hearing B. Failure behavior of precracked concrete beams retrofitted with FRP. J Compos Constr, ASCE 1998;2(3):138–44.
[11] Triantafillou TC, Plevris N. Strengthening of RC beams with epoxy-bonded fibre-composite materials. Mater Struct 1992;25:201–11.
[12] Lam L, Teng JG. Design-oriented stress–strain model for FRP-confined concrete. Constr Build Mater 2003;17:471–89.
[13] Maalej M, Tanwongsval S, Paramasivam P. Modeling of rectangular RC columns strengthened with FRP. Cem Concr Compos 2003;25:263–76.
[14] Gergely I, Pantelides CP, Nuismer RJ, Reaveley LD. Bridge pier retrofit using fiber-reinforced plastic composites. J Compos Constr, ASCE 1998;2(4):165–74.
[15] Eurocode-8. Design of structures for earthquake resistance, Part 3: Strengthening and repair of buildings. European Standard, EN 1998-3, Doc CEN/TC250/SC8/N343, Draft No. 32003.
[16] Di Ludovico M, Manfredi G, Mola E, Negro P, Prota A. Seismic behavior of a full-Scale RC structure retrofitted using GFRP laminates. J Struct Eng, ASCE 2008;134(5):810–21.
[17] Di Ludovico M, Prota A, Manfredi G, Cosenza E. Seismic strengthening of an under-designed RC structure with FRP. Earthquake Eng Struct Dyn 2008;37:141–62.
[18] Au C, Büyüköztürk O. Effect of fiber orientation and ply mix on fiber reinforced polymer-confined concrete. J Compos Constr, ASCE 2005;9(5):397–407.
[19] Gunes, O. Failure modes in structural applications of fiber-reinforced polymer (FRP) composites and their prevention. In: Developments in fiber-reinforced polymer (FRP) composites for civil engineering. Uddin N, editor. Cambridge (UK): Woodhead Publishing; 2013.
[20] Colomb F, Tobbi H, Ferrier E, Hamelin P. Seismic retrofit of reinforced concrete short columns by CFRP materials. Compos Struct 2008;82:475–87.
[21] Balsamo A, Colombo A, Manfredi G, Negro P, Prota A. Seismic behavior of a full-scale RC frame repaired using CFRP laminates. Eng Struct 2005;27:769–80.
[22] Pampanin S, Bolognini D, Pavese A. Performance-based seismic retrofit strategy for existing reinforced concrete frame systems using fiber-reinforced polymer composites. J Compos Constr, ASCE 2007;11(2):211–26.
[23] Zou XK, Teng JG, De Lorenzis L, Xia SH. Optimal performance-based design of FRP jackets for seismic retrofit of reinforced concrete frames. Composites: Part B 2007;38:584–97.
[24] Galal K, El-Sokkary H. Analytical evaluation of seismic performance of RC frames rehabilitated using FRP for increased ductility of members. J Perform Constr Facil 2008;22(5):276–88.
[25] Garcia R, Hajirasouliha I, Pilakoutas K. Seismic behavior of deficient RC frames strengthened with CFRP composites. Eng Struct 2010;32:3075–85.
[26] Gunes O, Tumer R, Gunes B, Faraji S. Performance-based seismic retrofit design for RC frames using FRP composite materials. To appear in Struct Eng Mech; 2013, submitted for publication.
[27] Saatcioglu M, Razvi S. Strength and ductility of confined concrete. J Struct Eng, ASCE 1992;118(6):1590–607.
[28] Freeman SA. Review of the development of the capacity spectrum method. ISET J Earthquake Technol 2004;41(1):1–13.
[29] ATC. Evaluation and improvement of inelastic seismic analysis procedures (ATC-55). California: Applied Technology Council; 2001.
[30] Bank LC. Debonding of FRP plated concrete: a tri-layer fracture treatment. Composites for construction structural design with FRP materials. John Wiley and Sons, Inc.; 2006.
[31] Au C, Büyüköztürk O. Debonding of FRP plated concrete: a tri-layer fracture treatment. Eng Fract Mech 2006;73(3):348–65.
[32] Laio A, Gervasio FL. Metadynamics: a method to simulate rare events and reconstruct the free energy in biophysics, chemistry and material science. Rep Prog Phys 2008;71(12):126601.
[33] Laio A, Parrinello M. Escaping free-energy minima. Prog Natl Acad Sci USA 2002;99(20):12562.
[34] Lau D, Büyüköztürk O, Buehler MJ. Characterization of the intrinsic strength between epoxy and silica using a multiscale approach. J Mater Res 2012;27(14):1787–96.
[35] Lau D. Debonding in bi-layer material systems under moisture effects: a multiscale approach. Cambridge: Massachusetts Institute of Technology; 2012.
[36] Tuakta C, Büyüköztürk O. Deterioration of FRP/concrete bond system under variable moisture conditions quantified by fracture mechanics. Compos Part B: Eng 2011;42:145–54.
[37] Lau D, Büyüköztürk O. Fracture characterization of concrete/epoxy interface affected by moisture. Mech Mater 2010;42(12):1031.
[38] De Castro J, Keller T. Design of robust and ductile FRP structures incorporating ductile adhesive joints. Compos Part B: Eng 2010;41(2):148–56.
[39] Anyfantis KN. Finite element predictions of composite-to-metal bonded joints with ductile adhesive materials. Compos Struct 2012;94(8):2632–9.
[40] Antonopoulos CP, T TC. Analysis of FRP-Strengthened RC beam-column joints. J Compos Constr, ASCE 2002;6(1):41–51.
[41] Bousselham A. State of research on seismic retrofit of RC beam-column joints with externally bonded FRP. J Compos Constr, ASCE 2010;14(1):49–61.
[42] Polies W, Ghrib F, Sennah K. Rehabilitation of interior reinforced concrete slab-column connections using FRP sheets. Constr Build Mater 2010;24:1272–85.
[43] Gunes O, Büyüköztürk O, Karaca E. A fracture-based model for FRP debonding in strengthened beams. Eng Fract Mech 2009;76(12):1897–909.
[44] Gunes O. A fracture based approach to understanding debonding in FRP bonded structural members. Cambridge: MIT; 2004.
[45] Büyüköztürk O, Hearing B. Crack propagation in concrete composites influenced by interface fracture parameters. Int J Solids Struct 1998;35(31–32):4055–66.
[46] Hearing B. Delamination in reinforced concrete retrofitted with fiber reinforced plastics. Cambridge: Massachusetts Institute of Technology; 2000.